



# Analysis of Mechanical Properties of Long-span Reinforced Concrete Composite Slabs under Different Splicing Methods

Liu Hai <sup>a\*</sup>

<sup>a</sup> CCTEG Chongqing Engineering (GROUP) CO., Ltd. China.

## Author's contribution

The sole author designed, analyzed, interpreted and prepared the manuscript.

## Article Information

DOI: 10.9734/JERR/2022/v22i317525

## Open Peer Review History:

This journal follows the Advanced Open Peer Review policy. Identity of the Reviewers, Editor(s) and additional Reviewers, peer review comments, different versions of the manuscript, comments of the editors, etc are available here: <https://www.sdiarticle5.com/review-history/84811>

Original Research Article

Received 09 January 2022  
Accepted 11 March 2022  
Published 17 March 2022

## ABSTRACT

Based on the long-span slab in an assembled building project, ABAQUS is used to simulate the mechanical properties and failure modes of the slab under the condition of the whole span cast-in-place slab and the two-way rebar truss composite slab (hereinafter referred to as composite slab) with different splicing methods, in which the slabs adopt fixed support and the slab loads are uniformly distributed load. The finite element simulation results show that the integrity and mechanical properties of the whole span cast-in-place slab are not different from those of the parallel splicing two-way composite slab, but they are obviously better than the parallel cross splicing two-way composite slab; In the same slab span, the cast-in-place seam of the composite slab in the middle cracks first due to stress concentration, and with the increase of the uniformly distributed load of the slab, the crack will pass through the cast-in-place seam and develop to the composite slab on both sides, and finally all the concrete at the bottom of the slab will crack and fail. According to the simulation results, the following suggestions are given: if the truss rebar composite slab is adopted for the long-span slab, the two-way composite slab should be adopted, and the cast-in-place seam should be arranged in the direction of less stress, and the seam should not be arranged in both directions.

Keywords: large-span; compositeslab; mechanical property; ABAQUS; plastic damage.

## 1. INTRODUCTION

Composite slab is a kind of prefabricated slab composed of precast bottom slab and cast-in-place reinforced concrete. The prefabricated bottom slab is not only a part of the slab, but also a permanent formwork for the cast-in-place reinforced concrete layer, which reduces the amount of cast-in-place and formwork erection, improves the efficiency and saves the construction period.

At present, there have been lots of researches on the shear strength, short-term stiffness, crack resistance and deflection of the composite slab at home and abroad [1-7], but the research on the mechanical properties of the composite slab under different splicing methods is slightly insufficient, especially when the slab span is large, the joint mode directly affects the bearing capacity and seismic performance of the composite slab. Furthermore, document stipulates that “prestressed concrete precast slab should be used for composite slab with span greater than 6m” [7], but it is not clear whether truss rebar can be used for composite slab when the slab span is greater than 6m. Therefore, it is urgent to carry out a series of research on large-span composite slabs.

Based on the above two research gaps, combined with the particularity of the slab of an assembled building project, the finite element

simulation of a large-span slab in the project is carried out by using ABAQUS, the mechanical properties of the composite slab under different splicing methods are analyzed, and compared with the integral cast-in-place slab, so as to lay a theoretical foundation for the follow-up design and construction work.

## 2. DESIGN OF COMPOSITE SLAB

The large-span slab is taken from an actual project. As shown in Fig.1, the span is 8000mm×9000mm and the thickness is 220mm. The rebars are double layers two-way rebars whose specification is 10@150. If the composite slab is adopted, the thickness of the prefabricated bottom slab is 60mm and the thickness of the cast-in-place layer is 160mm.

According to the relevant provisions of documents [7-8], the slab adopts two-way composite slab, the width of post cast seam between slabs is 300mm, and the anchorage length of stressed rebar at the bottom of precast slab extending into the cast-in-place splicing seam is 290mm. The rebar of single two-way composite slab is shown in Fig. 2.

The rebar truss is a kind of truss with rebar as the upper chord, lower chord and web member, which is connected by resistance spot welding. The rebar truss is shown as Fig.3.

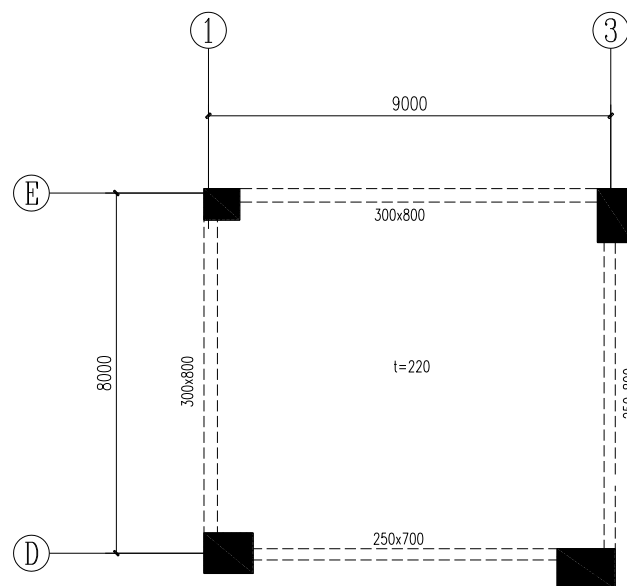


Fig.1. The large-span slab of a project

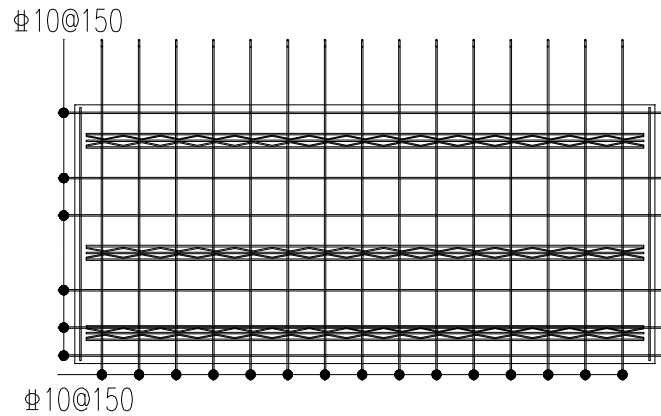


Fig.2. The rebar drawing of composite slab

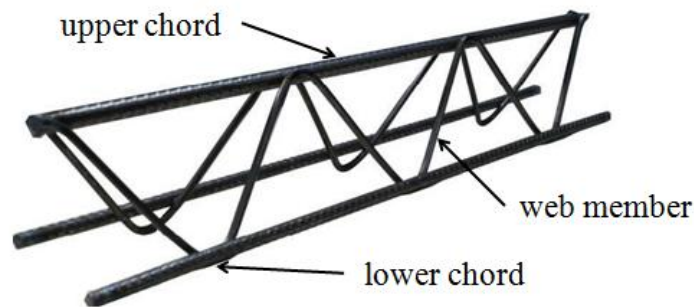


Fig.3. The sketch map of rebar truss

### 3. ANALYSIS MODEL OF ABAQUS

At present, there are two types of reinforced concrete finite element models: separated model and integral model. The separated model is to model the rebar and concrete respectively, that is to say the concrete is simplified into solid elements, and the rebar is simplified into beam elements or truss elements. The bonding and sliding between rebar and concrete can be simulated by setting contact relationship or adding corresponding interface elements. The integral model disperses the rebar in the whole element according to the proportion of the rebar in the element. The calculation cost of the whole model is the lowest and the accuracy is low. In this paper, the strain distribution and plastic damage of rebar and concrete need to be simulated respectively, so the separated model with high accuracy is adopted.

#### 3.1 Elements Type

Concrete is an isotropic material, which can be considered as a uniform solid element. In ABAQUS, the eight node hexahedral element C3D8R can be used for simulation. This element

has two properties: tensile cracking and crushing; The rebar can be simulated by two node linear truss element T3D2, which can only bear the action of uniaxial tension and pressure.

#### 3.2 Material Constitutive Parameters

The simulated rebar can be regarded as an ideal elastic-plastic material, and the plastic damage model is adopted for concrete. The model of slab rebar is HRB400 (grade III steel), the strength grade of concrete is C30, the measured yield strength of rebar is 472MPa, and the measured standard value of concrete axial compressive strength is 22.8MPa. According to "code for design of concrete structures GB50010-2010" [9], the constitutive parameters of rebar and concrete can be obtained, that is, the elastic modulus of concrete is taken as  $2 \times 10^4 \text{N/mm}^2$ , and the Poisson's ratio is taken as 0.2; The elastic modulus of rebar is taken as  $2 \times 10^5 \text{N/mm}^2$ , and the Poisson's ratio is taken as 0.3.

The double linear constitutive model is selected for rebar and the plastic damage model is selected for concrete, and the development or crushing of concrete cracks can be judged by plastic damage parameters. In the process of

ABAQUS simulation, the plastic damage parameters will reduce the stiffness matrix of concrete after damage, so as to achieve the purpose of simulating the damage evolution process of concrete, and can accurately reproduce the failure process of tensile cracking or crushing of concrete materials. Therefore, the introduction of plastic damage parameter is of great significance to explore the mechanical failure characteristics of composite slabs.

Appendix C of “code for design of concrete structures Gb50010-2010” gives the calculation method of tensile damage parameter  $d_t$  and compression damage parameter  $d_c$ , as shown in formula (1) ~ formula (5).

In the above formula,  $f_{t,r}$  and  $f_{c,r}$  respectively represent the representative value of concrete uniaxial tensile strength and the representative value of concrete uniaxial compressive strength, the value of  $f_{t,r}$  is 2.01mpa, and the measured

value of  $f_{c,r}$  is 22.8MPa;  $\varepsilon_{t,r}$  and  $\varepsilon_{c,r}$  respectively represent the peak tensile strain and compressive strain corresponding to the representative value of uniaxial tensile strength and uniaxial compressive strength, the corresponding values are  $9.52 \times 10^{-5}$  and  $1.52 \times 10^{-3}$ ;  $\alpha_t$  and  $\alpha_c$  respectively represent the parameter values of the descending section of the stress-strain curve of concrete under uniaxial tension and compression, which can be obtained according to the linear interpolation method, and then the values of  $\alpha_t$  and  $\alpha_c$  are taken as 1.26 and 0.92 respectively.

Guo [10] and others obtained the tensile stress-strain curve of concrete through the material property test, as shown in Fig.4. At the same time, they gave the location of each key point and the crack width of corresponding concrete when the concrete was damaged, as shown in Table 1.

$$d_t = \begin{cases} 1 - \rho_t [1.2 - 0.2x^5] & x \leq 1 \\ 1 - \frac{\rho_t}{\alpha_t (x-1)^{1.7} + x} & x > 1 \end{cases} \quad (1)$$

$$\sigma = (1 - d_t) E_c \varepsilon, \quad x = \frac{\varepsilon}{\varepsilon_{t,r}}, \quad \rho_t = \frac{f_{t,r}}{E_c \varepsilon_{t,r}} \quad (2)$$

$$d_c = \begin{cases} 1 - \frac{\rho_c n}{n-1+x^n} & x \leq 1 \\ 1 - \frac{\rho_c}{\alpha_c (x-1)^2 + x} & x > 1 \end{cases} \quad (3)$$

$$\sigma = (1 - d_c) E_c \varepsilon, \quad x = \frac{\varepsilon}{\varepsilon_{c,r}}, \quad \rho_c = \frac{f_{c,r}}{E_c \varepsilon_{c,r}} \quad (4)$$

$$n = \frac{E_c \varepsilon_{c,r}}{E_c \varepsilon_{c,r} - f_{c,r}} \quad (5)$$

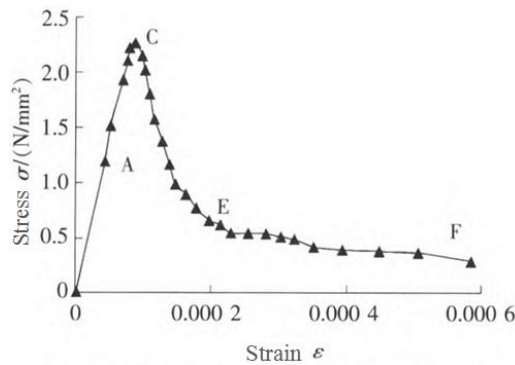


Fig. 4. The Tensile stress-strain curve of concrete

**Table 1. Quantitative description of concrete cracks under different stress stages**

Key point	Crack condition	crack width /mm	$d_t$
0~A~C~E	initial cracking	0.04~0.08	<0.6
E~F	crack development	0.1~0.2	0.6~0.92
after point F	crack penetration	>0.2	>0.92

### 3.3 Contact and Boundary Conditions

Because the expansion coefficients of rebar and concrete are similar, and the ribbed rebar can enhance the bonding performance with concrete, the simulation process considers that the relative slip between rebar and concrete can also be ignored, and the embedded region command can be used to restrict them together; At the same time, it is considered that the deformation of the prefabricated bottom plate of the composite slab is coordinated with that of the cast-in-place layer. According to a lot of experimental studies, the artificial roughening treatment on the surface of the prefabricated bottom plate and the existence of truss rebars make the composite slab will not undergo shear failure before bending failure. Therefore, it can be considered that there is no relative slip between the prefabricated bottom plate and the cast-in-place layer, In the process of simulation, the prefabricated base plate and cast-in-place layer can be bound together with the “tie” command.

Considering that in the actual project, the composite slab needs to be laid on the beam first (the bending stiffness and torsional stiffness of the beam are large), and then poured concrete to

form a whole. It can be seen from the literature [11] that the error of the calculation method of the slab according to the fixed support of four sides is small, so the boundary condition of the composite slab is set as the fixed support of four sides, That is, 6 degrees of freedom (3 translational degrees of freedom + 3 rotational degrees of freedom) need to be constrained.

### 3.4 Load Application

Apply a uniformly distributed load perpendicular to the slab, and the amplitude increases monotonically from 0kN/m<sup>2</sup> to 60 kN/m<sup>2</sup> until the slab is completely damaged.

### 3.5 Model Building

Based on the above theoretical basis and modeling experience, the whole span cast-in-place slab model (hereinafter referred to as model A), parallel splicing two-way composite slab model (hereinafter referred to as model B) and parallel cross splicing two-way composite slab model (hereinafter referred to as model C) are established respectively, as shown in Fig. 5.

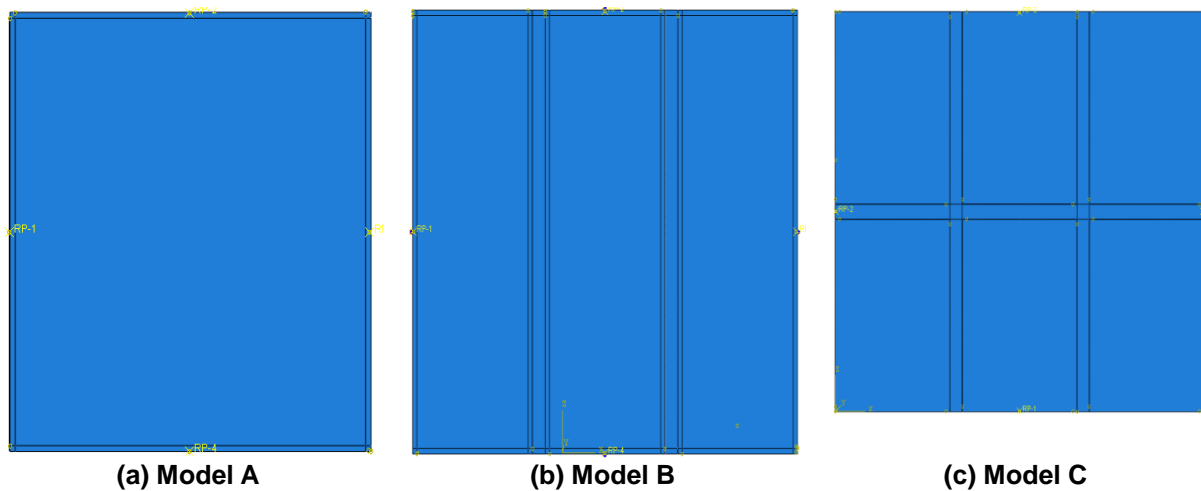


**Fig. 5. Schematic diagram of composite slab with different splicing methods**

## 4. FINITE ELEMENT ANALYSIS RESULTS

### 4.1 Displacement Analysis

According to the Chinese engineering standard—“code for design of concrete structures GB50010-2010”, when the slab span meets  $7\text{m} \leq l_0 \leq 9\text{m}$ , the allowable deflection limit is  $l_0 / 250$ , that is, when the slab span is 8m, the allowable deflection limit is  $8000\text{mm} / 250 = 32\text{mm}$ , and the slab uniformly distributed load corresponding to the allowable deflection limit is the ultimate load.

Selecting the point with the largest deflection in the slab span and extracting the load displacement curve, as shown in Fig.6. The damage of concrete at the bottom of slab under ultimate load is shown in Fig.7.

It can be seen from Fig.6 that with the increase of the uniformly distributed load on the slab, the displacement of the mid-span of the slab

increases. When approaching the allowable deflection limit, if the load continues to increase, the displacement will have a sudden change. In general, under the same slab load, the mid span displacement of model A is the smallest, the model B is the second, and the model C is the largest. The ultimate load that model A can bear is about  $25\text{kN/m}^2$ . At this time, the concrete at the bottom of the slab is almost cracked. Continue loading will cause the mid span displacement change suddenly, it is very easy to cause the brittle failure of the slab; The ultimate load that model B can bear is very close to that of model A at about  $24\text{kN/m}^2$ , and at this time, almost all the bottom of the mid span composite slab is cracked, and it develops towards the side span composite slab and along the direction of splicing seam, and the area of concrete crack is obviously more than that of cast-in-place slab; The ultimate load that model C can bear is about  $15.8\text{kN/m}^2$ , which is about 2/3 of the other two kinds of slabs. If the load continues, the mid span displacement will increase sharply. At this time, all the concrete in the tensile area at the bottom of the slab will crack and fail.

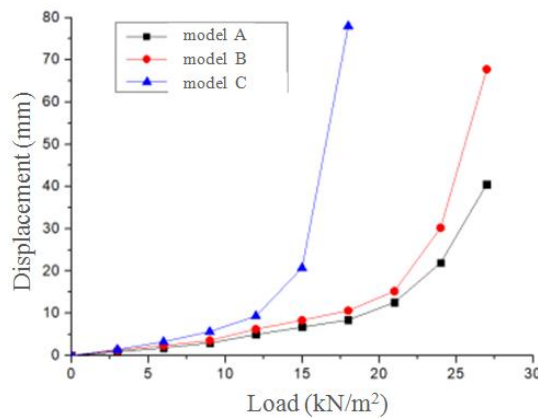


Fig.6. The midspan load-displacement curve of three kinds of slabs

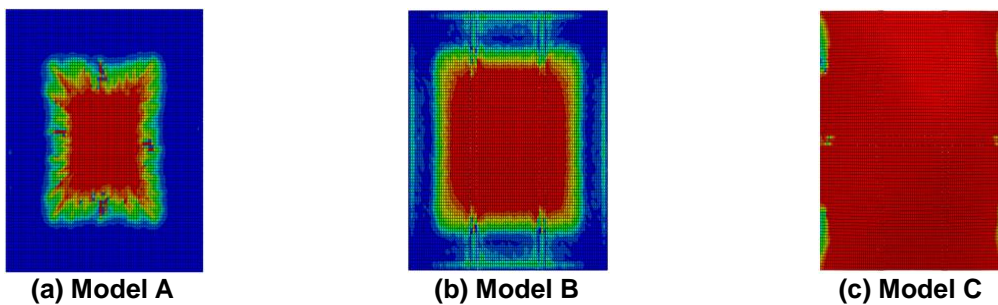


Fig.7. Plastic damage of the bottom of slab under ultimate load

To sum up, the seismic performance and integrity of composite slab are not as good as cast-in-place slab, but this gap will decrease with the increase of span. The reason is that the existence of truss rebar and anchor rebar will improve the integrity of the composite slab, but the more the post cast splicing seam is divided or divided in two directions, it will lead to the decline of the bearing capacity of the composite slab. Therefore, the post cast splicing seam of composite slab should be divided in one direction and arranged at the position with less stress.

## 4.2 Damage Analysis

### 4.2.1 Model A

The cloud diagram of damage distribution of cast-in-place slab is shown in Fig.8. It can be seen from the figure that in the initial cracking stage, with the increase of load, damage begins to appear at the middle of the bottom span of the cast-in-place slab, and there is no visible crack at the bottom of the slab. At this time, the uniformly distributed load of the slab is about  $9\text{kN/m}^2$ ; With the increase of external load, the slab enters the crack development stage. There are  $0.1 \sim 0.2\text{mm}$  penetrating cracks at the bottom of the slab along the long side, and cracks visible to the naked eye in other directions. At this time, the maximum value of  $d_t$  can reach 0.90, and the corresponding slab uniform load is about  $21\text{kN/m}^2$ ; As the load continues to increase, the slab enters the crack penetration stage. At this time, there are penetrating cracks greater than  $0.2\text{mm}$  in all directions at the bottom of the

slab, the value of  $d_t$  generally greater than 0.92, and the uniformly distributed load on the slab also reaches  $25\text{kN/m}^2$ . At this time, it is considered that all the concrete at the bottom of the slab has failed.

### 4.2.2 Model B

The cloud diagram of damage distribution of model B is shown in Fig.9. It can be seen from the figure that in the initial cracking stage, with the increase of load, damage begins to appear at the middle of the bottom span of the slab, and there is no visible crack at the bottom of the slab, with the maximum value of  $d_t$  at about 0.1. At this time, the uniformly distributed load on the slab is about  $9\text{kN/m}^2$ ; With the increase of external load, the slab enters the crack development stage, the through cracks whose width values  $0.1\sim 0.2\text{mm}$  appear in the mid span composite slab, and the visible cracks appear in the side span composite slab. At this time, the maximum value of  $d_t$  can reach 0.90, and the corresponding slab uniform load is about  $21\text{kN/m}^2$ ; As the load continues to increase, the slab enters the crack penetration stage. At this time, the crack of the mid span laminated plate passes through the post cast splicing seam and develops to the side span composite slab. There are penetrating cracks greater than  $0.2\text{mm}$  in all directions at the bottom of the slab, generally the value of  $d_t$  is greater than 0.92, and the uniformly distributed load on the slab also reaches  $24\text{kN/m}^2$ . At this time, it is considered that all the concrete at the bottom of the slab has failed.

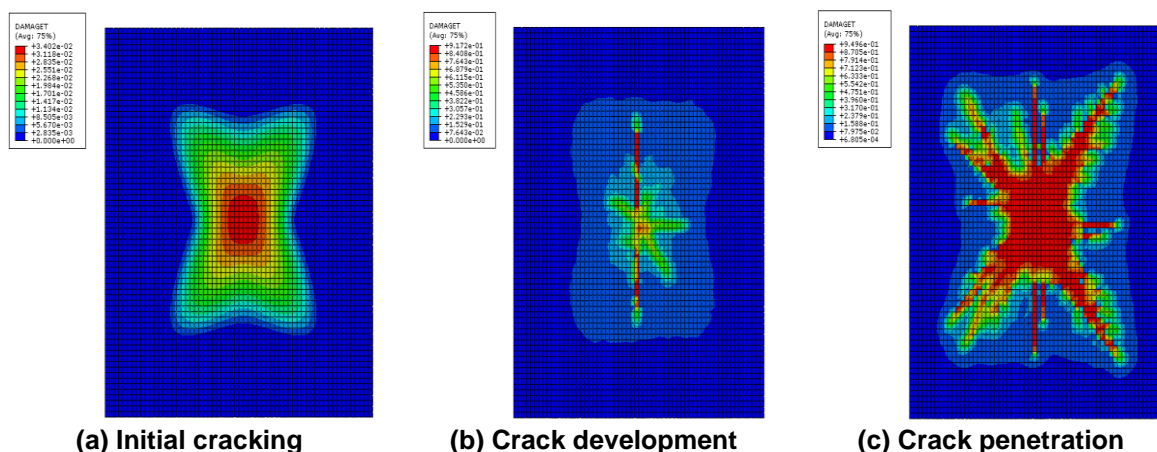


Fig. 8. Damage distribution in different stress stages of model A

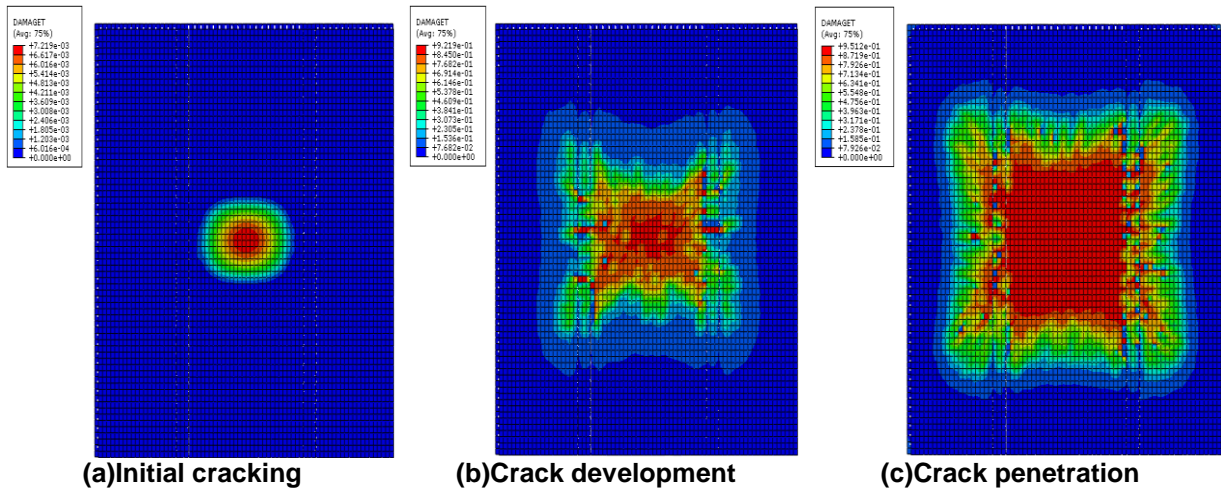


Fig. 9. Damage distribution in different stress stages of model B

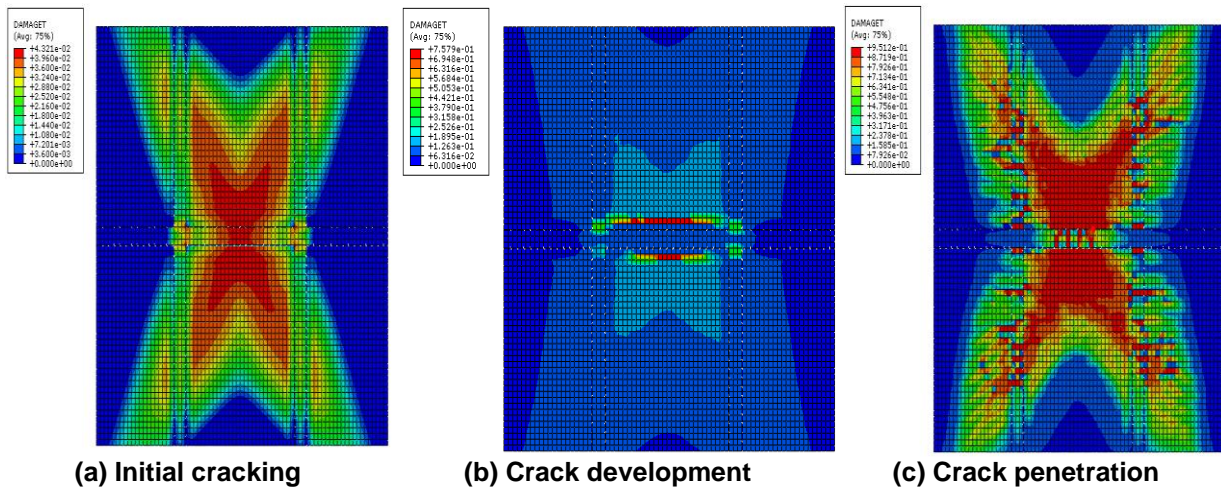


Fig. 10. Damage distribution in different stress stages of model C

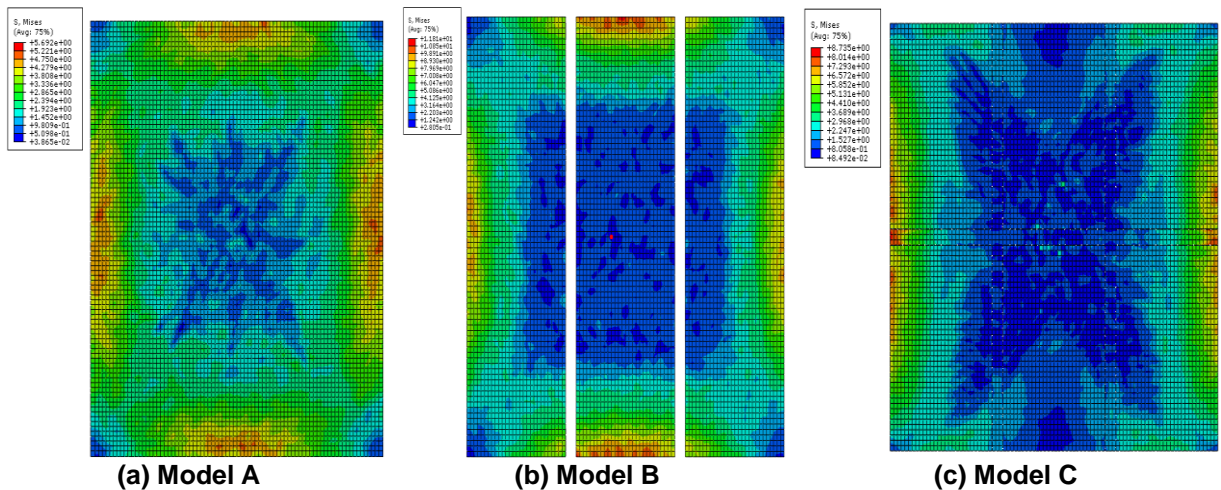


Fig. 11. Stress distribution of three kinds of slabs in cracks penetration stage

### 4.2.3 Model C

The cloud diagram of damage distribution of model C is shown in Fig.10. It can be seen from the figure that in the initial cracking stage, with the increase of load, damage begins to appear at the middle of the bottom span of the slab, and there is no visible crack at the bottom of the slab, with the maximum value of  $d_t$  at about 0.2. At this time, the uniformly distributed load on the slab is about  $6\text{kN/m}^2$ ; With the increase of external load, the slab enters the crack development stage, through cracks with the width of  $0.1\sim 0.2\text{mm}$  appear in the middle span composite slab along the short side splicing seam direction, and there are almost no cracks in the side span composite slab; As the load continues to increase, the slab enters the crack penetration stage. At this time, the crack of the mid span composite slab passes through the post cast splicing seam and develops to the side span composite slab. There are penetrating cracks greater than  $0.2\text{mm}$  in all directions at the bottom of the slab, but the most serious cracks are the two composite slabs in the middle span, with the maximum value of  $d_t$  reaching 0.95 and the uniformly distributed load on the slab reaching  $15\text{kN/m}^2$ . At this time, it is considered that all the concrete at the bottom of the slab is invalid.

### 4.3 Stress Analysis

The cloud diagram of stress distribution for the three kinds of slabs in the crack penetration stage is shown in Fig.11. It can be seen from the figure that in the crack penetration stage of cast-in-place slab, the maximum stress is concentrated around the slab. The reason is that the four sides of the slab are fixedly supported, and the edge of the slab is in a compression state. With the increase of load, the compressive stress gradually increases; At the same time, the maximum tensile stress at the bottom of the slab is always concentrated in the middle of the span or around the splicing seam, and an obvious stress concentration area is formed between the splicing seam, which is also in line with the above damage analysis results. The splicing seam is always the weak area of the composite slab. The number of splicing seams should be reduced and arranged at the position with less stress as far as possible.

## 5. RESULTS AND DISCUSSION

Based on the large-span slab encountered in a fabricated building project, ABAQUS is used to simulate the mechanical properties and failure forms of the slab when the slab adopts the whole span cast-in-place slab and the two-way composite slab with different splicing methods. The following conclusions are obtained from the finite element simulation results:

(1) Under the same load, the mid span displacement of the whole span cast-in-place slab is the smallest, the parallel spliced two-way composite slab is the second, and the parallel cross spliced two-way composite slab is the largest; At the same time, the ultimate load of the whole span cast-in-place slab is about  $25\text{kN/m}^2$  which shows the best integrity; Due to the setting of parallel splicing seam, the ultimate load of parallel spliced two-way composite slab is about  $24\text{kN/m}^2$ , which is not much different from the former and shows good integrity; However, due to the two-way joint of parallel cross spliced two-way composite slab, the integrity of the composite slab is poor, and the ultimate load is about  $15.8\text{kN/m}^2$ , which is at about 1/3 lower than the first two kinds of slabs;

(2) With the increase of external load, plastic damage appears at the bottom of the slab. Due to the existence of splicing seam in the composite slab, stress concentration is easy to occur in this area. In particular, the strain at the splicing seam of the middle span composite slab is the largest, and the plastic damage occurs first. With the increase of the external load, the crack begins to pass through the post pouring splicing seam and develop to the side span composite slab, and finally form a through crack, and the concrete at the bottom of the slab fails under tension;

(3) When the slab span is  $6\sim 8\text{m}$ , it is recommended to adopt the two-way composite slab, and the post cast splicing seam shall be set in the direction of less stress, and the two-way splicing seam shall not be set.

## 6. CONCLUSION

It is concluded that combination with the particularity of slab of a assembled building project, the finite element simulation of a large-span slab in the project is carried out by using ABAQUS, the mechanical properties of the composite slab under different splicing methods

are analyzed, and compared with the integral cast-in-place slab, so as to lay a theoretical foundation for the follow-up design and construction work.

## DISCLAIMER

The products used for this research are commonly and predominantly use products in our area of research and country. There is absolutely no conflict of interest between the authors and producers of the products because we do not intend to use these products as an avenue for any litigation but for the advancement of knowledge. Also, the research was not funded by the producing company rather it was funded by personal efforts of the authors.

## COMPETING INTERESTS

Author has declared that no competing interests exist.

## REFERENCE

1. Bayasi Z , Kaiser H , Gonzales M. Composite Slabs with Corrugated SIMCON Deck as Alternative for Corrugated Metal Sheets [J]. Journal of Structural Engineering, 2001,127(10):1198-1205.
2. Izzuddin BA , Tao XY , Elghazouli AY. Realistic Modeling of Composite and Reinforced Concrete Floor Slabs under Extreme Loading. I: Analytical Method [J]. Journal of Structural Engineering. 2004;130(120):1972-1984.
3. Sang Aihua, Lin Yuanzheng. Research and application of prestressed thin plate composite slab [J]. Architectural Technology. 1984;(11):2-4+6-9.
4. GuoQijun. Several problems in the design and construction of fly ash silicate industrial wallboard [J].Industrial Construction. 1984(07):27-30.
5. Xu Youlin, Jiang Hong, GuoShaoxian. Inspection of structural performance of double reinforced composite slab [J]. Architectural Technology. 1993;(12): 727-730.
6. Ling Ru, Zhou Haichao. Experiment Study on Bearing Performance of Different Types of Stitching Laminated Slabs [J].Journal of Anyang Institute of Technology, 2016, 15(02):37-39+68.
7. Technical specification for precast concrete structures: JGJ 1-2014 [ S ] . Beijing: China Architecture & Building Press; 2014. ( in Chinese)
8. Composite slab with lattice girders (60 mm precast slab): 15G366-1 [ S ] .Beijing: China Planning Press; 2015. ( in Chinese)
9. Code for design of concrete structures: GB 50010-2010 [ S ] . Beijing: China Architecture & Building Press; 2010. (in Chinese)
10. GUO ZH , ZHANG X. Experimental Investigation of Complete Stress-Deformation Curves of Concrete in Tension [J].Journal of Building Structures. 1988;84(4):278-285.
11. Yan JP, Guo BY. A collocation method for initial value problems of second-order ODEs by using laguerre functions [ J ] .Number Math Theory Method Application, 2011;4(2):283-295.

© 2022 Hai; This is an Open Access article distributed under the terms of the Creative Commons Attribution License (<http://creativecommons.org/licenses/by/4.0>), which permits unrestricted use, distribution, and reproduction in any medium, provided the original work is properly cited.

*Peer-review history:*

*The peer review history for this paper can be accessed here:  
<https://www.sdiarticle5.com/review-history/84811>*